

Seismoacoustic bottom inversion with AUV towed streamers: a multi-stage approach

Cristiano Soares, Sérgio M. Jesus, Agni Mantouka and Paulo Felisberto
LARSyS, University of Algarve, Campus de Gambelas, 8005-139 Faro, Portugal
{csoares, sjesus, amantouka, pfelis}@ualg.pt

Abstract—The WiMUST (Widely scalable Mobile Underwater Sonar Technology) Project envisions using a team of autonomous underwater vehicles towing short acoustic arrays for seismic surveying of seabottom geoacoustic properties. One of the objectives in the project is to tackle the inversion of acoustic data collected with short towed horizontal arrays by means of a Matched-Field Inversion (MFI) technique. While there is great deal of experience in MFI and the so-called focalization applied to horizontal propagation scenarios, in near vertical propagation scenarios, with a source receiver horizontal distance limited to a few tens of meter or less, there is little understanding in terms of feasibility of the acoustic inversion of bottom properties. In particular, the simultaneous inversion of bottom properties (soundspeeds, densities, attenuations) of multiple bottom layers needs to be tackled, since the experimenter has to account for the admissible mismatch of other environmental properties such as water soundspeed and depth, and the potential solution ambiguity inherent to an optimization problem with ten or more unknown parameters. The actual simulation study, carried out with an environmental scenario and geometric set up based on the Peljesac data set, considers a shallow water acoustic propagation scenario with a short array. A sensitivity analysis in MFI provides understanding on the observability of the unknown parameters of interest. A mismatch analysis indicates that watercolumn mismatch (soundspeed and depth) may cause the MFI procedure to break down. Based on the conclusions taken from the sensitive and mismatch analysis, an iterative acoustic inversion concept with feedback of intermediate parameter estimates is developed and tested with simulated data.

I. INTRODUCTION

The WiMUST (Widely scalable Mobile Underwater Sonar Technology) project envisions using a team of autonomous underwater vehicles (AUVs) towing acoustic arrays (streamers), in seismic reflection surveying, instead of using vessel towed streamers of hydrophones, for acquisition of seabottom reflected acoustic signals. One of the main advantages of this concept is that the set of streamers towed by a team of AUVs may be seen as an acoustic antenna with reconfigurable geometry (enabled by the physical decoupling of vessel and streamers). In order to achieve a payload compatible with AUV operation, that concept requires streamers of short aperture with a reduced number of hydrophones - e.g. 8-element arrays with a 1 m spacing.

This concept includes the acoustic inversion of the geoacoustic properties of multiple seabottom layers by means of Matched-Field Inversion (MFI). While the seismic industry employs seismic arrival-time based processing for bottom estimation, the scientific community has produced an extensive literature on model based or MFI techniques, over the past two

decades [1], [2]. MFI is a model based inversion technique where field data collected with an acoustic array is compared with replica fields computed with an acoustic propagation model for hypothetical values of unknown search parameters. In order to carry out this procedure a certain degree of *a priori* knowledge on the environmental properties of the acoustic channel is required for model input or acoustic inversion guidance (e.g. for setting the parameter search intervals). The model input is a realistic description of the acoustic propagation channel, including water depth, water soundspeed, seabottom layers thickness, densities, attenuations, etc. Accurate knowledge on the source/receiver geometry is necessary for a viable forward modelling procedure. When the available knowledge on some parameter is inaccurate then that parameter shall be included as a free search parameter in the optimization procedure.

Although the acoustic inversion is posed as a global optimisation problem by means of a Genetic Algorithm (GA), in order to allow a search for several unknowns, still it may be computationally cumbersome, as in a scenario with several layers, the number of unknown parameters may rise to 12 or more, whereas the sensitivity of the field may vary significantly from one geophysical property to the other, and/or from one seabottom layer to the other, rendering varying degrees of estimation uncertainty, even under good match between data and replica fields. In a large search space, including unknowns such as layer thickness, soundspeed, density, and attenuation over several layers, a parameter hierarchy of strong and weak influence on the received acoustic field shall be taken into account in terms of *a posteriori* uncertainty.

The main objective of this study is to understand whether simultaneous acoustic inversion for multiple seabottom layers is viable by means of MFI in the WiMUST scenario. This implies inspecting field sensitivity for the set of physical parameters and to model mismatch studies in order to understand its impact on the viability of the inversion procedure. This is necessary, for example, to understand the impact of model mismatch of water column soundspeed and depth on the viability of the acoustic inversion, and the accuracy required in direct measurements or historical data of these properties.

This paper develops an algorithm for the environmental inversion of seismic data, as to respond to the requirements of the WiMUST Project. The development reported herein aims at understanding basic requirements to enable acoustic inversion of seismic data collected with a short horizontal

array with a short emitter receiver array horizontal distance in a shallow water scenario (30 m watercolumn), for determining seabottom properties over multiple layers.

The other aspect exploited herein is the possibility of breaking the inversion problem into smaller inversion problems, where each inversion problem includes a subset of unknowns, for example, to some degree separate strong from weak parameters, or, more specifically, to separate parameters of different layers. The terms *strong* and *weak* are used to express the position of a property in the parameter hierarchy.

Finally, in order to obtain *a priori* knowledge for MFI guidance, a Least Squares estimator for layer soundspeed and thickness based on travel times only is derived. This step is to acquire *a priori* information on these parameters without the constraints and implications of using a full acoustic propagation model. That information can provide a rough representation of the physical model, and can be used to set up the acoustic inversion procedure, e.g. set up parameter search intervals.

This paper is mainly a simulation study that uses a canonical scenario based on the Peljesac data set (Croatia, 2015), for generating synthetic acoustic data. In section II the data model and two match-field processors are given. In section III a simulation study is carried out, covering a sensitivity and a model mismatch analysis; this section includes an iterative global optimization test with a genetic algorithm. Finally, experimental results on layer depth and velocity analysis with the Least Squares Estimator are provided in section V. Section VI provides conclusions of the actual study and gives directions for future work.

II. BOTTOM PARAMETER INVERSION WITH MFI

Matched-Field Inversion (MFI) is an acoustic inversion technique for the estimation of watercolumn and seabottom properties [2], [3]. MFI was derived from Matched-Field Processing (MFP), which originally was proposed for range and depth source localisation [4], [5], [6]. In MFP a measured field is compared to model replicas calculated for hypothetical source positions within a specific range and depth search region to form an ambiguity surface whose maximum will indicate the location of the acoustic source, provided that the underlying physical model is sufficiently accurate. The comparison between the field and the replicas is done by means of a processor which usually is a correlation function based on statistical assumptions made on signal and noise. Since the acoustic signal is used as an intermediate observable to estimate source location, MFP can be considered to be an inverse problem. MFI is similar to MFP, but the objective is to infer on the physical properties of the acoustic propagation channel, with known source and receiver geometry.

In this section the broadband data model and two matched-field processors are reviewed. The broadband data model has been previously seen as contribution to alleviate the ill-conditioning often posed in acoustic inversions with an increased number of unknowns. By exploiting field coherence across the spectral band, additional information can be

retrieved from the spectral components, which in turn can contribute for coping with the ambiguity over the search space, by means of sidelobe attenuation.

The matched-field processors considered herein are the broadband (BB) conventional or Bartlett processor [6], [7], and the BB minimum-variance (MV) processor [8], [6], [7]. While the conventional processor has been preferred for being robust against model mismatch, its major limitation is its poor resolution and sidelobe suppression. The minimum-variance processor has been seen as high-resolution method, with an increased ability for attenuating sidelobes in comparison to the Conventional processor.

A. The broadband data model

The broadband data model for the acoustic data received at an L -receiver array is written as a concatenation of K narrowband signals $\underline{Y}(\omega_k)$ at discrete frequencies of interest ω_k :

$$\begin{aligned}\underline{Y} &= [\underline{Y}^T(\omega_1), \dots, \underline{Y}^T(\omega_k), \dots, \underline{Y}^T(\omega_K)]^T \\ &= \mathbf{H}(\underline{\theta})\tilde{\underline{S}} + \underline{N}\end{aligned}\quad (1)$$

in order to introduce, as much as possible, a common framework for the narrowband and broadband cases (see Ref. [9] for a detailed discussion). This data model allows for accounting for field coherence across frequencies. Vector $\underline{\theta}$ represents the channel parameters and matrix $\mathbf{H}(\underline{\theta})$ is the channel response matrix given as

$$\mathbf{H}(\underline{\theta}) = \begin{bmatrix} \underline{H}(\omega_1, \underline{\theta}) & \cdots & \underline{0}_{k-1} & \cdots & \underline{0}_{K-2} \\ \underline{0}_1 & \cdots & \underline{H}(\omega_k, \underline{\theta}) & \cdots & \underline{0}_1 \\ \underline{0}_{K-2} & \cdots & \underline{0}_{K-k} & \cdots & \underline{H}(\omega_K, \underline{\theta}) \end{bmatrix}, \quad (2)$$

where the $\underline{H}(\omega_k, \underline{\theta})$ is an L -vector representing the channel response at frequency $\omega_k, k = 1, \dots, K$. $\underline{0}_k$ is a vector with kL zeros. This channel matrix is analogous to that used in classical array processing models for multiple emitters. In the present case, each column is relative to a frequency ω_k , however, the channel vectors do not overlap across the columns, in order to keep frequencies separated. The channel matrix has KL rows, and K columns. The vector $\tilde{\underline{S}}$ has entries $S(\omega_k)\alpha(\omega_k)$, i.e., the source spectrum multiplied by a random perturbation factor at each frequency $\omega_k \in [\omega_1, \omega_K]$. The random perturbation factor $\alpha(\omega_k)$ appears as an attempt to account for unmodeled ocean inhomogeneities [9]. The vector \underline{N} represents the noise, which is assumed Gaussian zero mean, and follows the same notation as \underline{Y} in eq. (1). Let

$$\mathbf{C}_{YY} = E\{\underline{Y}\underline{Y}^H\} = \mathbf{H}\mathbf{C}_{SS}\mathbf{H}^H + \sigma_N^2\mathbf{I} \quad (3)$$

be a generic definition of the spectral density matrix (SDM) for \underline{Y} defined in (1), where \mathbf{C}_{SS} is the signal matrix given by $E\{\tilde{\underline{S}}\tilde{\underline{S}}^H\}$, and σ_N^2 the noise variance. The dimensions of the SDM \mathbf{C}_{YY} are $KL \times KL$ consisting of $L \times L$ cross-frequency SDMs $\mathbf{C}_{YY}(\omega_{k_1}, \omega_{k_2})$. The SDMs for $k_1 \neq k_2$ are noiseless according to (3) since it is assumed that the noise is uncorrelated both across space and frequency. Concerning the signal component, if the received signal are fully coherent,

than it just happens that $\mathbf{C}_{SS} = \underline{S} \underline{S}^H$, which has rank equal to one. On the other hand, if the emitted waveform is a random signal, then $\mathbf{C}_{SS} = \text{diag}[\sigma_S^2(\omega_1), \dots, \sigma_S^2(\omega_k), \dots, \sigma_S^2(\omega_K)]$, with $\sigma_S^2(\omega_k) = E\{\alpha^*(\omega_k)\alpha(\omega_k)S^*(\omega_k)S(\omega_k)\}$. In that case the rank of the signal matrix is equal to K . Note that for this case the SDM \mathbf{C}_{YY} is a matrix with blocks only in the diagonal. The intermediate case is that where the rank of the signal matrix can vary between 1 and K , representing partial frequency cross-correlation.

B. The BB Bartlett processor

Conventional or Bartlett matched-field processors are the most popular in underwater acoustic estimation problems, since they have been used in virtually every study on MFP. The frequency domain Bartlett processor, also called linear processor, performs matched-field beamforming by weighting the output of the array elements at different frequencies and summing over all elements:

$$P_B(\theta) = E\{\text{tr}[\mathbf{W}^H(\theta)\underline{Y}(\theta_0)\underline{Y}^H(\theta_0)\mathbf{W}(\theta)]\}, \quad (4)$$

where \mathbf{W} is a weighting matrix with K columns. Note that it is assumed that the acoustic field is zero mean without loss of generality. Replacing with (3) and by performing a few ordinary algebra steps to maximize this criterion with respect to $\mathbf{W}(\theta)$ under the constraint $\text{tr}[\mathbf{W}^H(\theta)\mathbf{W}(\theta)] = 1$ the following function is obtained:

$$P_B(\theta) = \frac{\text{tr}[\mathbf{H}^H(\theta)\mathbf{C}_{YY}\mathbf{H}(\theta)\mathbf{C}_{SS}]}{\text{tr}[\mathbf{H}^H(\theta)\mathbf{H}(\theta)\mathbf{C}_{SS}]}. \quad (5)$$

This is the BB Bartlett processor for generic assumptions on the emitted signal component in terms of the cross-frequency structure. Other functions can be obtained by working out assumptions on \mathbf{C}_{SS} comprehending either uncorrelated either fully correlated frequency components.

C. The BB minimum-variance processor

The Bartlett processor has generally important limitations in terms of sidelobe attenuation. This might become a major difficulty in multi-parameter estimation problems, when several unknown parameters are considered. As an attempt to alleviate such limitation Capon [8] proposed a processor commonly known as Minimum Variance processor. The derivation of the broadband MV processor is well documented in the literature [10] and follows a similar notation as that for the BB Bartlett processor above resulting as

$$P_{MV}(\theta) = \frac{\text{tr}[\mathbf{H}^H(\theta)\mathbf{H}(\theta)\mathbf{C}_{SS}]}{\text{tr}[\mathbf{H}^H(\theta)\mathbf{C}_{YY}^{-1}\mathbf{H}(\theta)\mathbf{C}_{SS}]}. \quad (6)$$

With regard to calculations, the MV processor presents the need to invert the SDM \mathbf{C}_{YY} , which can be done in a straightforward fashion provided that the SDM is of rank KL . In practice, this requires the number of snapshots of the received signal \underline{Y} to be equal or larger than KL for calculating the sample SDM. Otherwise, it may be necessary to diagonal overload the SDM, as suggested in [11].

III. SIMULATION RESULTS

A. The Peljesac scenario

The Peljesac scenario is based on a site off the Croatian coast where a seismic survey has been conducted, and whose environmental and geometric setup was used for the simulation tests [12]. Figure 1 shows a representation of the environmental model used for acoustic data simulations with the OASES acoustic propagation model [13], which is called Canonical Model. The watercolumn is 30 m deep with a soundspeed of 1500 m/s. The depths of the layers' interfaces are based results obtained by GeoSurveys on the Peljesac data set [12], while the seabottom parameters were taken from Ref. [14]. Seabottom layer 1 was set to silt, layer 2 to sand, and layer 3 to moraine.

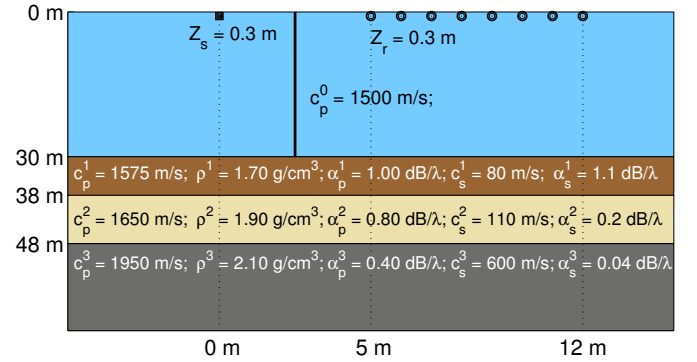


Fig. 1. Peljesac Canonical Model: water column over a three-layer seabottom.

Both the source and the receivers are at 0.3 m depth. In this study, a 8-element array with a 1 m spacing is considered, instead of the array aperture and element spacing of the streamers used in the Peljesac experiment. The pulse transmitted during that experiment has a duration less than to 2 ms and a 4 kHz bandwidth, which allows the bottom reflections to arrive after the direct arrival has been dissipated. However, in a narrowband case, under this geometry, in the first receiver elements the direct arrival may interfere significantly with the bottom reflected arrivals if these are too close, leading to impossible parameter discrimination of the parameter values in matched-field inversions. It was observed that, for a 5 m array offset, that interference would be sufficiently reduced to allow proper matched-field inversions.

Figure 2 shows the impulse response simulated with the OASES propagation model [13] for the scenario depicted in Figure 1 for a receiver array with elements from 2 to 100 m range with 1 m spacing. The frequency band is 200 to 4000 Hz, sampling time was set to 0.1 ms and the window length was 4096 samples. There are the direct arrival and several groups of four arrivals. The direct arrival is associated to a surface reflected arrival. For hydrophones close to the source, an energy leaking effect is observed over the entire impulse response duration, which is attributed to the sidelobe structure of the pair of direct and surface reflected arrival, under the bandwidth and length of impulse response considered for acoustic compu-

tations. The direct arrival becomes attenuated with increasing range due to cancelling with the surface reflected arrival, whose delays tend to equalise with increasing range. The first three groups are reflections from the three bottom interfaces, and each group contains bottom reflected, bottom-surface reflected, surface-bottom reflected, and surface-bottom-surface reflected arrivals. The vertical two-way source-receiver travel time of the first reflection is $59.4/1500 = 39.6$ ms, the travel time for the second is $39.6 + 16/1575 = 49.8$ ms, and for the third is $49.8 + 20/1650 = 61.9$ ms.

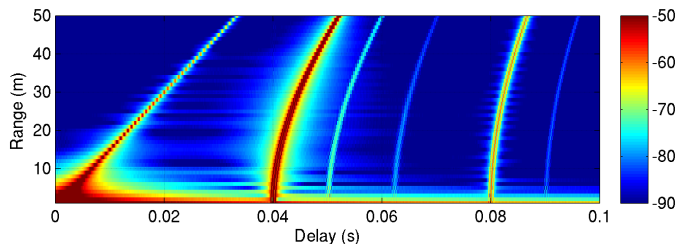


Fig. 2. Envelope of the of the modelled impulse response for source-receiver ranges from 2 to 50 m in the Canonical Case, computed with the OASES acoustic model. Field computations were carried out for a frequency band 200 to 4000 Hz, sample time 0.1 ms, and frequency response with 4096 frequency bins. The color scale is given in dB.

IV. SENSITIVITY AND MISMATCH ANALYSIS

In this section the sensitivity of the acoustic field to variations on seabottom parameters will be inspected on the Canonical Model given in section III-A. More specifically, the field generated for the given true parameter values is compared to the field generated for hypothetical model parameters by means of the matched-field processors given in section II in order to understand to which degree the parameters can be discriminated by the conventional and MV processors, and to understand the amount of influence of each parameter in the acoustic field.

A. Sensitivity analysis

The sensitivity analysis is carried out with the Canonical Case, considering a 8-element horizontal array, and frequencies 400, 500, and 600 Hz, both for the Conventional processor given in eq. (5) and the MV processor given in eq. (6). The simulation considers full frequency coherence, meaning that the signal matrix is filled with ones.

Figure 3 shows sensitivity curves for the geoacoustic parameters of the three layers of the given scenario. This test is to conclude about the observability of the parameters, and to compare the parameter discrimination enabled by the Conventional and the MV processors. Each row shows the parameters in seabottom layer i considered for inversion: compressional speed (c_p^i), density (ρ^i), and compressional attenuation (α_p^i). The black curves represent the MF response for the MV processor, and the gray curves represent the MF response for the conventional processor. As seen, it is apparent that the MV processor clearly outperforms the Conventional processor in terms of parameter discrimination, as the latter shows a

nearly flat response for most parameters, including the most influent parameters such as compressional speed and density. If the analysis is restricted to the MV processor, the result indicates that density and compressional speed can be well discriminated, although there is some loss in sensitivity with increasing layer. There is less sensitivity for compressional attenuation, with nearly no discrimination for attenuation in the third layer. It was observed that the shear parameters have no observable influence in any layer (not shown), and therefore these are not considered for acoustic inversion in the following sections.

The results shown in Figure 3 suggest that for the current geometric setup a high-resolution processor shall be employed in order to enable the MFI procedure to optimize the parameter vector.

B. Mismatch analysis

In the actual concept the main target is the estimation of properties of one or multiple seabottom layers. Some environmental information may be readily available with varying degree of accuracy. Bathymetric data is often readily available, and water soundspeed can be measured directly. Inaccurate knowledge of environmental properties can lead to model mismatch with varying impact on the inversion procedure or on parameter estimates. On the other hand, such environmental parameters can be jointly optimized with the target parameters, provided that some *a priori* information is available.

In this section the impact of mismatch in waterdepth and watercolumn soundspeed is inspected, in order to understand the minimum set up necessary in a global search, as to evaluate if ground truth data is sufficient or if these properties must be jointly optimized from the acoustic data. For this set of simulation tests the Canonical Case is used (see Figure 1).

Figure 4 shows ambiguity surfaces for soundspeed in the three seabottom layers against waterdepth obtained with the MV processor with a 8-element horizontal array for frequencies of 400, 500, and 600 Hz (with full spectral coherence). The result shows that for the actual environmental scenario, the effect of mismatch in the water depth is severe, since a departure from the true as small as 10 to 20 cm has a significant impact on the MF power in all cases, as it degrades significantly. Further testing on waterdepth mismatch has shown that when the soundspeeds of two interfacing layers are jointly searched, a biased estimate is obtained, i.e., an ambiguity enables the compensation of that error.

Sound speed in the water column can be measured during the acoustic shooting. However, it can change with time and location. Figure 5 shows ambiguity surfaces of watercolumn soundspeed c_p^0 against the soundspeed in the three seabottom layers c_p^1, c_p^2, c_p^3 . The true value of c_p^0 is 1500 m/s. The results indicate that an error in c_p^0 less than 5 m/s is sufficient to cause a significant shift of the other parameters or to cause the MF response to break down.

In this section, mismatch on watercolumn soundspeed and waterdepth have been inspected. The results indicate that an error within 1% in the waterdepth and less than 0.5% in

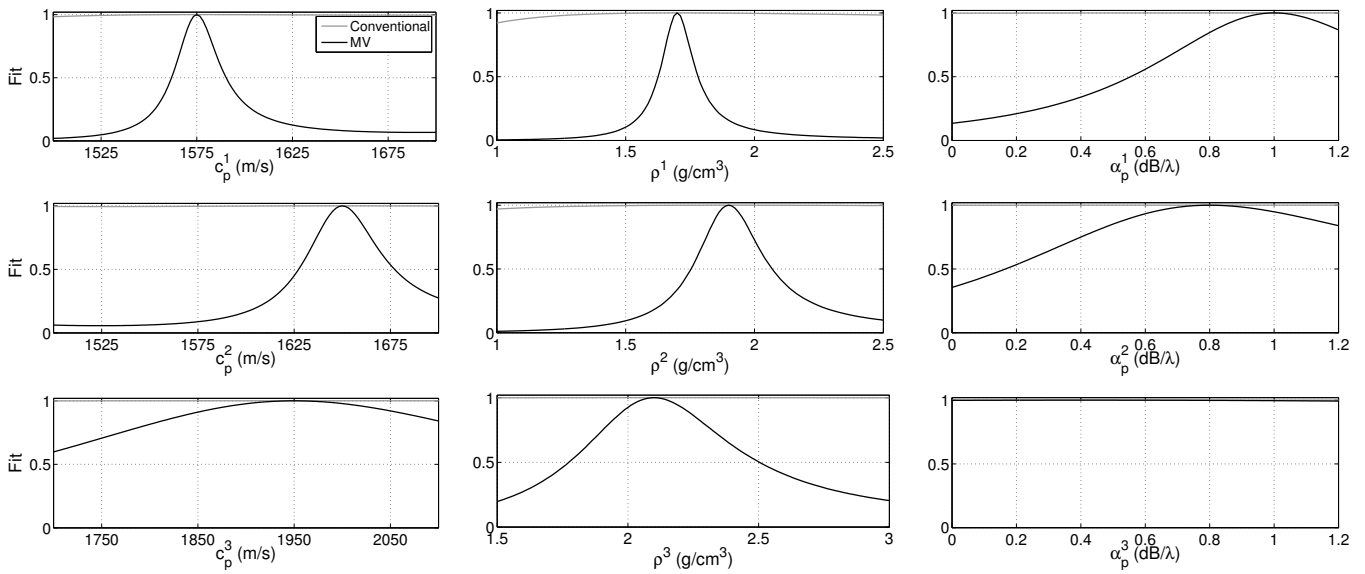


Fig. 3. Sensitivity curves for compressional speed (c_p^i), density (ρ^i), compressional attenuation (α_p^i). Layer 1 (top row); Layer 2 (middle row); Layer 3 (bottom row). Conventional processor (gray curves); MV processor (black curves).

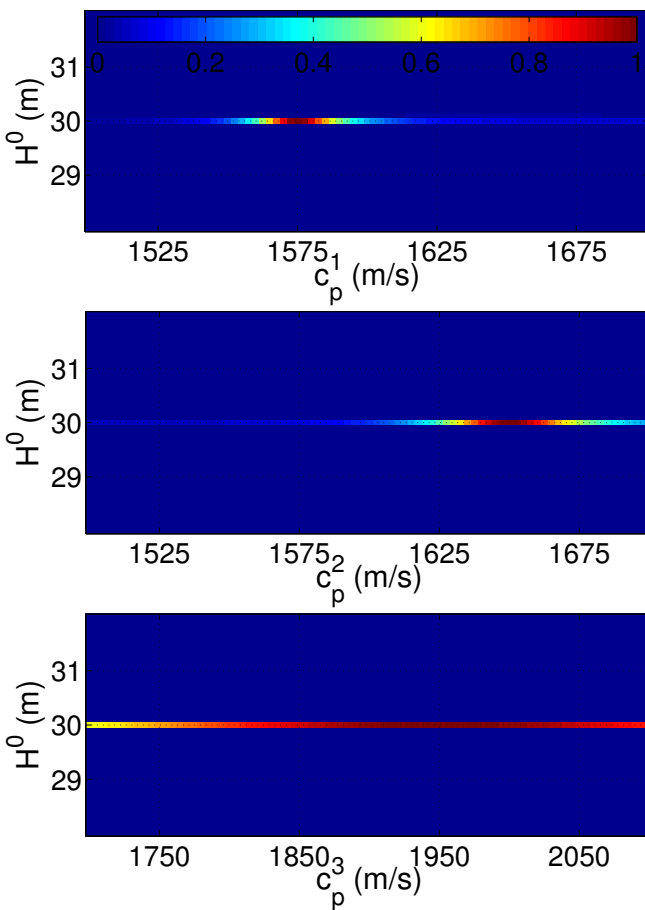


Fig. 4. Effect of water depth mismatch on compressional speed in the three bottom layers. Ambiguity surfaces obtained for the Canonical Case for 400, 500, and 600 Hz and a 8-element horizontal array, with the MV processor.

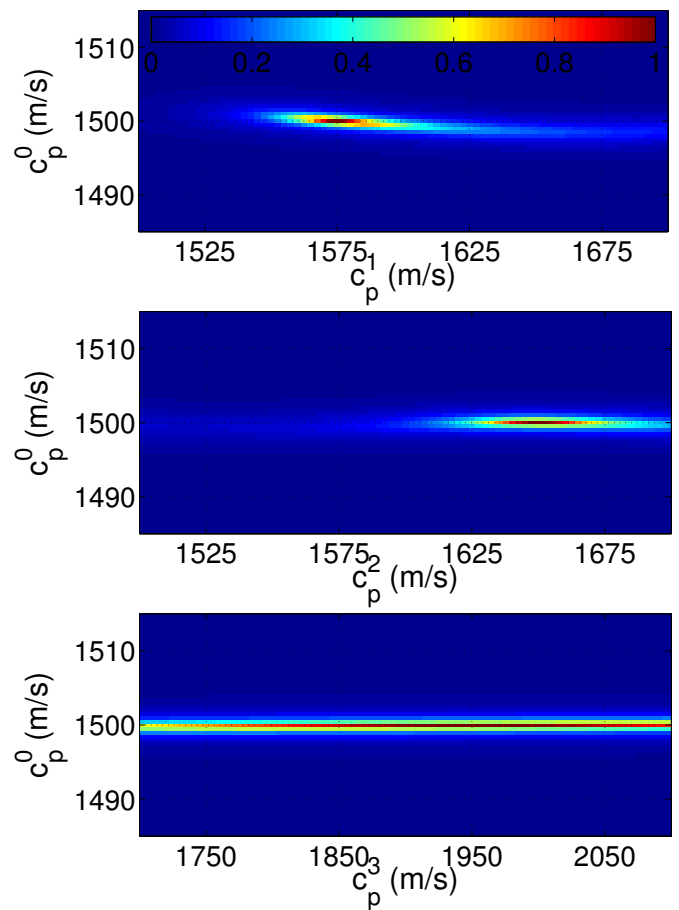


Fig. 5. Effect of watercolumn soundspeed mismatch on compressional speed in the three layers. Ambiguity surfaces obtained for the Canonical Case for 400, 500, and 600 Hz and a 8-element horizontal array, with the MV processor.

watercolumn sound speed may cause an inversion procedure to fail to produce a model adjustment. This suggests that it is likely that some uncertainty must be accounted for in the inversion by including these parameters as free unknowns.

C. Global optimization

1) *A posteriori statistics*: During the optimization process, the genetic algorithm generates samples of the search space, which can be used as a by-product. These samples can be used to estimate *a posteriori* probabilities of the parameter vectors observed during the global optimization process [1]. The probability of the k^{th} parameter vector is given by

$$\sigma(\underline{\theta}_k) = \frac{\exp[\phi(\underline{\theta}_k)/T]}{\sum_{k=1}^N \exp[\phi(\underline{\theta}_k)/T]} \quad (7)$$

where $\phi(\underline{\theta}_k)$ is the fit obtained for parameter vector $\underline{\theta}_k$, N is the number of observations of the parameter vector $\underline{\theta}$, and T is the average fit of the N observations. For the q^{th} parameter in the parameter vector $\underline{\theta}$ the marginal probability distribution for obtaining the value κ can be found by summing eq. (7) over all observations:

$$\sigma^q(\theta^q = \kappa) = \frac{\sum_{k=1}^N \exp[\phi(\underline{\theta}_k)/T] \delta(\theta_k^q = \kappa)}{\sum_{k=1}^N \exp[\phi(\underline{\theta}_k)/T]}. \quad (8)$$

The optimisation with the GA is stochastic search, that is initiated with a random population (set of hypothetical solutions). This means that each time, the optimisation evolves in a different way and convergence may be different each time. In order to increase the probability to approach the global maximum, several parallel independent populations are started. Herein, the observations of $\underline{\theta}$ used for the *a posteriori* statistics are the individuals of the last generation of multiple independent populations. Provided that the population converges to the true solution, those samples tend to be those fittest sampled during the evolution of the ensemble of parallel populations started. Here the estimate of the parameter vector is taken as the *a posteriori* mean vector, given as

$$E(\underline{\theta}) = \sum_{k=1}^N \underline{\theta}_k \sigma(\underline{\theta}_k). \quad (9)$$

2) *Inversion results: iterative global optimization*: In this section an iterative global optimization algorithm is proposed and tested on synthetic data. The iterative algorithm is to account for the large search space, by breaking the inversion problem into optimizations on subsets of unknowns. The main objective is to estimate the compressional speeds c_p^i , densities ρ^i , and compressional attenuations α_p^i , over seabottom layers $i = 1, 2, 3$. It is assumed that knowledge is available on the watercolumn soundspeed and the depths of the three layer interfaces, however, with some uncertainty. The iterative optimization algorithm consists in optimizing all or part of the parameter set in an iteration, and feed intermediate parameter estimates into the next iteration, where only a subset of the unknowns is to be optimized. The choice of parameter subsets is case dependent and somewhat *ad hoc*. The idea is to

Layer	θ_i
L ₀	c_p^0, H^0
L ₁	$c_p^1, \rho^1, \alpha_p^1, H^1$
L ₂	$c_p^2, \rho^2, \alpha_p^2, H^2$
L ₃	$c_p^3, \rho^3, \alpha_p^3$

Iteration	θ_i
1.	$[c_p^0, H^0]; [c_p^1, \rho^1, \alpha_p^1, H^1]; [c_p^2, \rho^2, \alpha_p^2, H^2]; [c_p^3, \rho^3, \alpha_p^3]$
2.	$[c_p^0, H^0]; [c_p^1, \rho^1, \alpha_p^1, H^1]; [c_p^2, \rho^2, \alpha_p^2, H^2]$
3.	$[c_p^2, \rho^2, \alpha_p^2, H^2]; [c_p^3, \rho^3, \alpha_p^3]$

Fig. 6. Set of unknown seabottom parameters, by layers (top); parameter subsets for iterative matched-field inversion (bottom).

Parameter	Low. bound	Up. bound	Q. steps
c_p^0 [m/s]	1480	1520	64
H^0 [m]	29	31	32
c_p^1 [m/s]	1525	1725	32
ρ^1 [g/cm ³]	1.0	2.5	32
α_p^1 [dB/λ]	0.0	1.2	16
H^1 [m]	37	39	32
c_p^2 [m/s]	1625	1825	32
ρ^2 [g/cm ³]	1.00	2.5	32
α_p^2 [dB/λ]	0.00	1.2	16
H^2 [m]	47	49	32
c_p^3 [m/s]	1750	2050	64
ρ^3 [g/cm ³]	1.5	3.0	32
α_p^3 [dB/λ]	0.00	1.20	16

TABLE I
SEARCH BOUNDS AND QUATIZATION STEPS FOR GLOBAL OPTIMIZATION WITH THE GENETIC ALGORITHM.

optimize upper layers and most influent parameters first. The number of iterations depends on the number of layers. Figure 6 shows the set of unknowns by layers (upper panel) by layer, and the selected subsets for iterative optimization with the genetic algorithm (lower panel). In the 1st iteration all parameters are optimized in order to generate intermediate estimates of parameters not included in the 2nd iteration. The mean values of the *a posteriori* distributions, taken as intermediate estimates, are fed into the next iteration. After the 1st iteration, parameter estimates of layers L₀ and L₁ are obtained in iteration 2; parameter estimates of layers L₂ and L₃ are obtained in iteration 3. Some layers appear repeated, as L₂ is included in all iterations, and L₃ is included in iterations 1 and 3. In a previous test, it was concluded that this is necessary in order to allow sufficient degrees of freedom for the search to evolve over the different dimensions of the solution space, and enable convergence to the true solution independently where the search is started when only a partial optimizations are carried out.

Table I shows the set of unknown parameters to be estimated in the actual test, with search bounds and number of quatization steps for each parameter. The size of the search

Parameter	True	Mean	MAP	ϵ_1	ϵ_2	ϵ_3
$c_p^0(m/s)$	1500	1498	1495	0.0	0.1	-
$H^0(m)$	30.0	29.97	29.90	0.1	0.1	-
$c_p^1(m/s)$	1575	1593	1577	1.2	1.1	-
$\rho^1(g/cm^3)$	1.70	1.69	1.73	7.3	0.4	-
$\alpha_p^1(dB/\lambda)$	1.00	0.94	1.12	0.7	6.4	-
$H^1(m)$	38.0	38.00	37.71	0.1	0.0	-
$c_p^2(m/s)$	1650	1700	1664	4.8	3.4	3.0
$\rho^2(g/cm^3)$	1.90	1.77	1.73	1.4	1.0	6.7
$\alpha_p^2(dB/\lambda)$	0.80	0.64	0.64	5.1	18	20
$H^2(m)$	48.0	48.36	48.48	0.7	1.1	0.8
$c_p^3(m/s)$	1950	1949	1926	3.7	-	0.1
$\rho^3(g/cm^3)$	2.10	1.82	1.74	1.0	-	13
$\alpha_p^3(dB/\lambda)$	0.40	0.40	0.16	84	-	0.5

TABLE II

ITERATIVE OPTIMIZATION RESULTS: TRUE PARAMETER VALUES; *a posteriori* DISTRIBUTIONS MEAN; MAXIMUM *a posteriori* (MAP); RELATIVE ERRORS OVER ITERATIONS.

space is approximately 1.8×10^{19} . The genetic algorithm was set to 40 generations with a size of 130 individuals in the first iteration and less individuals in the others; a cross over probability of 0.8 and a 45% individual mutation probability, with 10 independent populations. The cost function is the MV processor given in eq. (6) with a single frequency of 300 Hz. The spectral density matrix was generated as in eq. (3) with signal-to-noise ratio of 60 dB.

Table II summarizes the inversion results, showing true value, distribution mean and distribution maximum *a posteriori* (MAP), and relative errors ϵ_i , where subscript i stands for the iteration. The distribution mean has a relatively good adjustment with the true value. The MAP estimate provides a more accurate estimate for some parameters, but is less accurate in others. Concerning the relative error evolution over iterations it is seen that the compressional speeds c_p^i improved steadily, while the densities ρ^i show a less consistent behavior over iterations. In general, there is a good agreement since a reduced relative error was obtained, specially, in the watercolumn and first seabottom layer, and also in the third layer.

Figure 7 shows distributions of the fit obtained in last GA generation, respectively for the first second, and third iterations. The result indicates that in the first iteration (all parameters) the fits in the final generations are distributed over the whole interval with some prevalence for a fit of 0.9, but with a peak close to 0, and another peak at 0.7. In the second iteration there is some improvement, where a shift towards 0.9 is seen, and in the third iteration most individuals have a fit greater than 0.9. This suggests that there is a clear improvement in terms of match between the replica and field data at the end of the independent optimizations, although this is not clearly reflected in terms of parameter relative errors.

The *a posteriori* probability distributions are given in Figure 8. These distributions were obtained with eq. (8) using the individuals of the last three generations of the 10 independent populations, and for the final iteration where each parameter was included. The green mark indicates the true value of the parameter, and the red asterisk indicates the mean value of

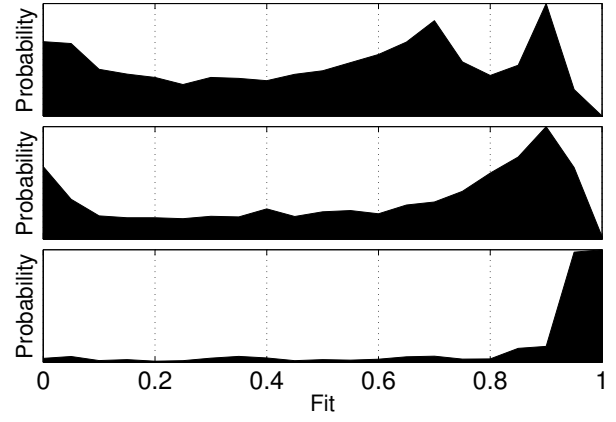


Fig. 7. Probability distribution of model fit over the first (top), second (middle), and third iterations (bottom). Model fits range from 0 to 1.

the distribution, computed with eq. (9), which is taken as the parameter estimate. The relative error shown in each plot is in regard to the distribution mean.

Densities and layer depths tend to be the most compact, while compressional speeds are relatively spread over the search interval. Nonetheless, the MAP of compressional speeds are in good agreement with the true value. It is apparent that distribution spread increases with layer. The degree of spreading in the compressional speeds are corroborated by the ambiguity surfaces of Figure 5, where it was already apparent that the sensitivity reduced with increasing depth.

V. PRELIMINARY RESULTS: DEPTH AND VELOCITY ANALYSIS

The configuration of the global optimization shown in section IV-C2 assumes a great deal of knowledge in waterdepth and bottom layer interface depths, by restricting the search to the uncertainty of parameter values obtained previously, rather than the full parameter value. Other parameters, such as compressional speed, require the choice of search intervals containing the true parameter values. Either case requires some *a priori* idea on the parameter value, for acoustic inversion guidance. *A priori* knowledge on the depths and sound speeds are useful for acoustic inversion guidance. This knowledge can be earned from a depth and velocity analysis based on equations that relate travel time, depth, and sound velocity [15].

In this section layer depth and velocity analysis is carried out for the Peljesac data set. First, a least squares estimator for layer depth and sound velocity is derived. Then depth and sound velocity analysis is carried out for the watercolumn and first seabottom layer for a small portion of the Peljesac data set.

A. Least-squares estimation for depth and velocity analysis

Let us consider the watercolumn, and a reflection from the water/seabottom interface. It is assumed that emitter and receiver are at the same depth, close to the water surface, and

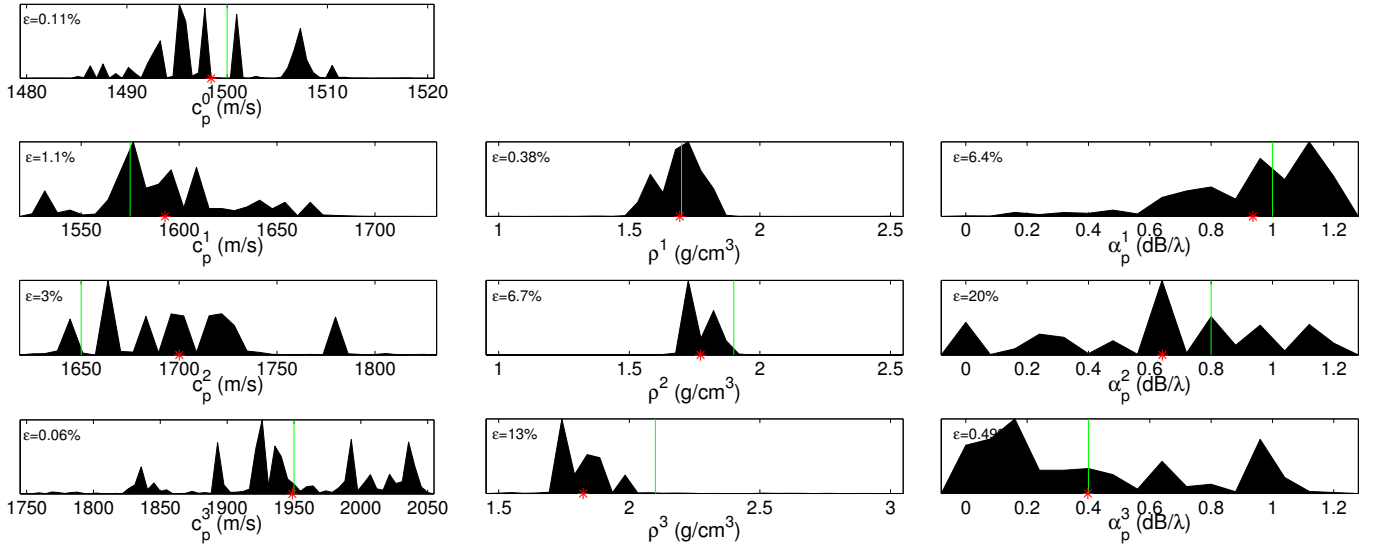


Fig. 8. Probability distributions obtained by sampling from a Boltzmann distribution for the geoacoustic parameters. The green bar indicates the true value and the red asterisk indicates the distribution mean. Depending on parameter, the distributions were taken from the second or third iteration.

that source-receiver horizontal distance is r , the travel time for the geometrical ray from emitter to receiver is given by

$$\tau = \frac{D}{c} = \frac{(4z^2 + r)^{\frac{1}{2}}}{c}, \quad (10)$$

where D is the total distance traveled by the ray, c is the wave speed, and z is the vertical distance between emitter and interface, i.e., layer thickness. This equation can be rewritten as

$$\tau^2 c^2 - 4z^2 = r^2. \quad (11)$$

In the actual framework, we are considering that wave speed c and layer thickness z as the unknowns of interest. Let us adopt the notation used so far, letting $c = c_p^0$ for soundspeed in water, and $z = H^0$ for water depth. If instead of one receiver, a L -element array of receivers is considered, then eq. 11 can be rewritten for the l^{th} receiver as

$$\tau_l^2 (c_p^0)^2 - 4(H^0)^2 = r_l^2 \quad l = 1, \dots, L, \quad (12)$$

where τ_l and r_l are the travel time, and the horizontal source-receiver range for the l^{th} receiver, respectively. This forms an overdetermined system of L equations (if $L > 2$), where the unknown variables are $(c_p^0)^2$ and $(H^0)^2$. This system can be written in matrix notation as

$$\mathbf{A}\underline{\Theta} = \underline{R} \quad (13)$$

where \mathbf{A} is a $L \times 2$ matrix with rows $[\tau_l^2, -4]$, $\underline{\Theta} = [(c_p^0)^2, (H^0)^2]^T$, and \underline{R} is a L -element vector with elements r_l^2 . The elements of $\underline{\Theta}$ can be determined by means of a Least Squares minimization, given in matrix notation as

$$\hat{\underline{\Theta}} = (\mathbf{A}^T \mathbf{A})^{-1} \mathbf{A}^T \underline{R}. \quad (14)$$

For a two-interface analysis, i.e., watercolumn and first seabottom layer, the depth and soundspeed analysis can be carried out by this approximation [15]:

$$\tau^2 \approx (T_1 + T_2)^2 + \frac{T_1 + T_2}{T_1 c_1^2 + T_2 c_2^2} r^2, \quad (15)$$

where T_1 and T_2 are the zero-offset travel times through first and second layers, respectively, and c_1 and c_2 are the soundspeed in first and second layers. This is a good approximation when the horizontal distance is less than layer depth. Otherwise the validity of this approximation may not hold. For a L -element horizontal array, and previous notation for compressional soundspeed in watercolumn and first seabottom layer, this equation can be rewritten as

$$\tau_l^2 = (T_1 + T_2)^2 + \frac{T_1 + T_2}{T_1 (c_p^0)^2 + T_2 (c_p^1)^2} r_l^2 \quad l = 1, \dots, L. \quad (16)$$

Once again, this forms an overdetermined system of L equations (if $L > 2$), where the unknowns are

$$\theta_1 = (T_1 + T_2)^2 \quad (17)$$

and

$$\theta_2 = \frac{T_1 + T_2}{T_1 (c_p^0)^2 + T_2 (c_p^1)^2}. \quad (18)$$

The equation system above can be given in matrix notation as

$$\mathbf{A}\underline{\Theta} = \underline{T} \quad (19)$$

where \mathbf{A} is a $L \times 2$ matrix with rows $[1, r_l^2]$, $\underline{\Theta} = [\theta_1, \theta_2]^T$ is a 2-element vector with the unknowns, and \underline{T} is a L -element vector with elements τ_l^2 . The elements of $\underline{\Theta}$ can be determined by means of a least squares minimization, given in matrix notation as

$$\hat{\underline{\Theta}} = (\mathbf{A}^T \mathbf{A})^{-1} \mathbf{A}^T \underline{T}. \quad (20)$$

The unknowns determined by this estimator are expressions containing unknown zero-offset travel times T_1 , T_2 . To determine these times, one assumes that depth and velocity estimates of the first layer are available, which means that T_1 and c_p^0 in eqs. (17) and (18) are known, and therefore these equations can be solved to determine T_2 and c_p^1 .

B. Depth and velocity analysis with the Peljesac data set

In this section the estimators for layer depth and velocity analysis given in eqs. (14) and (20) are applied to a portion of acoustic data from the Peljesac data set comprehending 100 shots. Acoustic shots were fired by a sparker every 0.6 s, therefore about 60 s of data are considered. In a previous step, not shown here, the travel times from source to receivers, for the first and second interfaces were estimated by correlating the received signal with an estimate of the emitted waveform. The streamer has 24 receivers, but for the actual test only receivers 2 to 16 were used.

Figure 9 shows the analysis results obtained for the watercolumn (a) and first seabottom layer (b). The results are in agreement with the estimates reported by GeoSurveys [12], i.e. 28 m for the watercolumn and 10 m for the first bottom layer. For this shot interval, in terms of distribution, the maximum count is obtained for 27 m for watercolumn, and 9.5 m for the first bottom layer. For soundspeed no previous information is available. The maximum distribution count was obtained for 1520 m/s in the first layer, and 2030 m/s in the second layer.

As a comment, it is observed that there is an interdependency of depth and soundspeed. Another feature is a periodicity of 3 shots observed. These results may be revised in the future, since the equations above consider a common mid point gather, which was not considered in the travel time processing.

VI. CONCLUSIONS

Among others, the objective of the WiMUST project is to develop a model based bottom inversion methodology for acoustic data collected on multiple short horizontal acoustic arrays towed by underwater vehicles.

The actual study analyses the matched-field inversion (MFI) regarding the acoustic inversion of field data collected with a towed horizontal array in a shallow water scenario considering a three layer seabottom. The main objective is to determine the depths of seabottom layers interfaces and the main geoacoustic properties. The source receiver geometry is such that nearly vertical acoustic propagation is being considered. This is a defining characteristic, in the sense that a reflection from each layer interface is being considered, and to what concerns the relation of travel delays to sound speed and depths of layer interfaces.

To understand the problem at hand, first the influence of each parameter in each layer was inspected, both in terms of match-field response and model mismatch. The sensitivity analysis indicates that compressional parameters and density of all layers are influent to propagation, while shear parameters

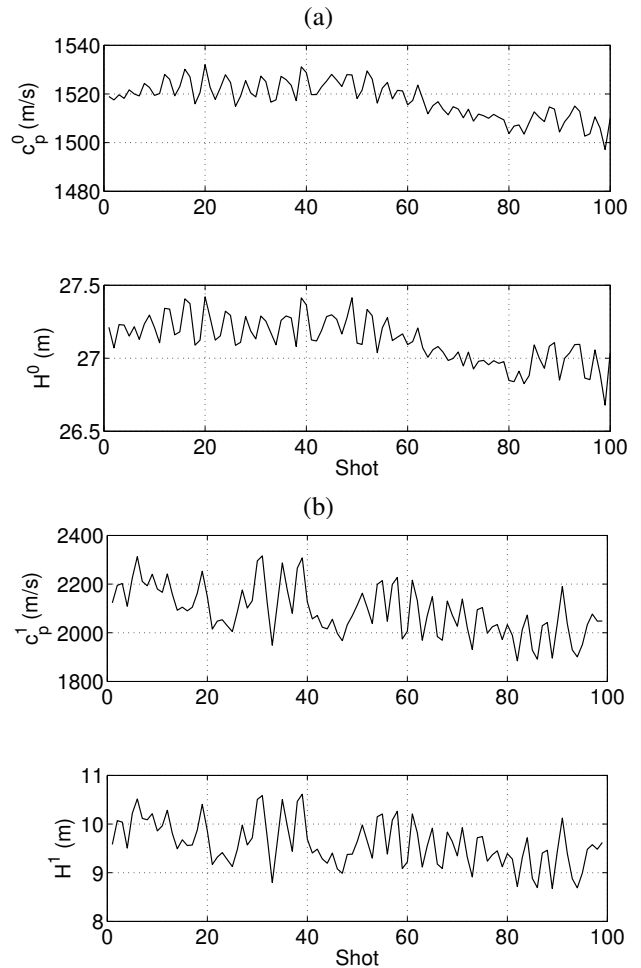


Fig. 9. Depth and velocity analysis for watercolumn (a) and first seabottom layer (b) obtained with the Least Squares Estimator based on travel times and source/receiver geometry.

are not, as expected. In other words, for the actual scenario shear speed and attenuation can not be inverted for by MFI.

The mismatch study has demonstrated that very small deviations on layer depths and water column sound speed can cause breakdown in MFI procedure. For example, an error in waterdepth as small as a few tens of centimetres may cause the MFI procedure to fail. A relative error within 1% in watercolumn soundspeed may cause the MFI procedure to fail. This analysis has also determined that in a MFI procedure watercolumn soundspeed and layer depths shall be included, even if *a priori* knowledge or direct measurements are available.

This renders the inversion problem very challenging, since a total of 13 parameters of four layers are to be included as free unknowns. Given that the number of unknowns may be potentially large, generally rendering a large search space (as large as 10^{19} possible solutions), an iterative optimisation procedure was tested. A previous test with nine unknown parameters case, where the inversion problem was broken into partial inversion problems of only two parameters with

successive feedback of intermediate solution into subsequent iterations, indicated that convergence to the true parameters is possible, provided that the search is initiated at a favourable position.

The iterative inversion was adapted to the global optimisation with the genetic algorithm, where the iterations consisted of a first iteration for all parameters of all layers, the second iteration for the parameters of the first and second seabottom layers, and the third iteration included the second and third seabottom layers. The result indicate that this approach allowed a significant overall fit improvement, and that most parameters tend to reduce the relative errors across iterations. Further, inspection indicated that adding more iterations is not effective with the current set up because the search space is still large and each iteration is a new search, whereas convergence to the true parameter is not assured such that the relative errors are undefinedly reduced.

The acoustic inversion performed herein did not perform a full inversion of the depths of the layer interfaces. It assumed that relatively accurate information, either layer depths or travel delays were readily available. Instead of blind search for layer depths, since nearly vertical propagation is being considered, travel times shall be obtained in a previous step. The travel times can be incorporated directly in the global search or one can previously obtain rough estimates for layer depths and soundspeeds. This information is useful for optimization guidance, as for providing aid in choosing the search intervals of these parameters. A least-squares estimator for layer depth and velocity analysis was implemented and applied to a small portion of the Peljesac data set. The estimates for the depths are in agreement with the seismic analysis reported by GeoSurveys.

The results obtained in this study suggest a seismic data inversion algorithm that is based on *a priori* estimates for layer depths and soundspeeds. This step shall provide waterdepth and depths of other layers that can be detected. Based on that information iterative global optimisation is performed for watercolumn and seabottom parameters, from the top layers to the bottom layers.

The next steps of this development require the simulation study to be completed, in particular, in the sense to improve convergence of the global optimization. One open question is whether feeding in intermediate MAP estimates and using multi-frequencies can improve convergence over iterations. Experimental work on the Peljesac data set shall be conducted aiming at the application of the geoacoustic inversion methodology proposed herein.

REFERENCES

- [1] P. Gerstoft, "Inversion of seismoacoustic data using genetic algorithms and *a posteriori* probability distributions," *J. Acoust. Soc. America*, vol. 95(2), pp. 770–782, 1994.
- [2] D. F. Gingras and P. Gerstoft, "Inversion for geometric parameters in shallow water: Experimental results," *J. Acoust. Soc. America*, vol. 97, pp. 3589–3598, 1995.
- [3] P. Gerstoft and D. Gingras, "Parameter estimation using multi-frequency range-dependent acoustic data in shallow water," *J. Acoust. Soc. America*, vol. 99(5), pp. 2839–2850, 1996.
- [4] M. J. Hinich, "Maximum-likelihood signal processing for a vertical array," *J. Acoust. Soc. Am.*, vol. 54, pp. 499–503, 1973.
- [5] H. P. Bucker, "Use of calculated sound fields and matched-detection to locate sound source in shallow water," *J. Acoust. Soc. Am.*, vol. 59, pp. 368–373, 1976.
- [6] A. B. Baggeroer, W. A. Kuperman, and P. N. Mikhalevsky, "An overview of matched field methods in ocean acoustics," *IEEE J. Ocean Eng.*, vol. 18, pp. 401–424, 1993.
- [7] A. Tolstoy, *Matched Field Processing for Underwater Acoustics*. Singapore: World Scientific, 1993.
- [8] J. Capon, "High-resolution frequency-wavenumber spectrum analysis," in *Proc. IEEE*, vol. 57(8), August 1969, pp. 1408–1418.
- [9] C. Soares and S. M. Jesus, "Broadband matched field processing: Coherent and incoherent approaches," *J. Acoust. Soc. Am.*, vol. 113, no. 5, pp. 2587–2598, May 2003.
- [10] C. Soares, S. M. Jesus, and E. Coelho, "Environmental inversion using high-resolution matched-field processing," *The Journal of the Acoustical Society of America*, vol. 122, no. 6, pp. 3391–3404, 2007.
- [11] K. Hsu and A. B. Baggeroer, "Application of the maximum-likelihood method (mlm) for sonic velocity logging," *Geophysics*, vol. 51, pp. 780–787, 1986.
- [12] H. Duarte, N. Alves, and A. Pinto, "Peljesac Bridge 3D Survey Data Processing Report," GeoSurveys, Technical Report REP54114, March 2016.
- [13] H. Schmidt, *OASES 3.1 - User guide and reference manual*, MIT, March 2011.
- [14] F. Jensen, W. Kuperman, M. Porter, and H. Schmidt, *Computational Ocean Acoustics*. New York: AIP Series in Modern Acoustics and Signal Processing, 1994.
- [15] G. Drijkoningen and D. Verschuur, "Seismic data processing (ta3600/tg001)," Centre for Technical Geoscience, Delft university of Technology, P.O. Box 5028, 2600 GA Delft, The Netherlands, Tech. Rep., 2003.

ACKNOWLEDGMENT

This work was funded under H2020 Research program of the European Union under project WiMUST contract ICT-645141.